

Biomimetic Crystallization of Apatite in a Porous Polymer Matrix

Karsten Schwarz and Matthias Epple*

Abstract: Hydroxyapatite and fluoroapatite were crystallized by double diffusion of two aqueous solutions into a pellet of porous poly(hydroxyacetic acid) (polyglycolide). Distinct morphologies were observed for these calcium phosphate phases. This suggests specific interactions between the growing aggregates and the polymeric matrix (nucleation and growth of crystals). Fluoroapatite gave elongated hexagonal prisms developing multiply branched edges that finally closed into spheres. Hydroxyapatite (from simulated body fluid, SBF) formed hexagonal terraces and compact elongated hexagonal prisms. Such composites of a biodegradable polymer and apatite phases are of interest as potential biomaterials, such as for bone replacement.

Keywords: apatite • biomineralization • crystal growth • materials science • polymers

Introduction

Biomimetic synthesis of inorganic compounds such as calcium carbonate, silicon dioxide, and apatite has gained increasing attention over the last few years.^[1–9] The major goal is to understand the specific interactions and processes that enable nature to form such sophisticated objects as radiolarians, eggshells, sea-urchin spines or bone. Such knowledge would be highly advantageous for the controlled preparation of micrometer-structured materials.

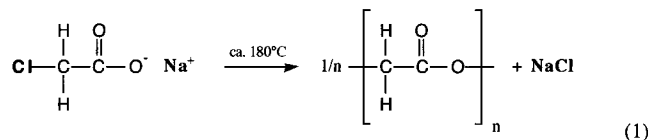
We were inspired by experiments reported recently by Kniep and Busch,^[1] who crystallized fluoroapatite in a collagen matrix. They employed a double diffusion technique in which stoichiometric solutions of CaCl_2 and $\text{Na}_2\text{HPO}_4/\text{KF}$ migrated into a gel to form a precipitate. The formation of fluoroapatite aggregates with distinct morphology was observed: elongated hexagonal prisms were formed whose ends started to branch into rods. After a number of generations resembling fractal growth, dumbbell-shaped aggregates were formed that finally closed into spheres. On the surface of these spheres, secondary radial growth as submicrometer-sized needles occurred. A special electrostatic interaction between the collagen matrix and the dipolar fluoroapatite crystals was assumed to be responsible for this unusual morphology.

We recently reported on the preparation of polyglycolide with high internal porosity and pore sizes in the micrometer

range and below.^[10–12] As polyglycolide is of considerable interest in medical technology, for example as bone substitute material or resorbable fixture,^[13–18] we adopted this method to prepare a porous polymer matrix filled with apatite. Such a composite would be especially advantageous for application as bone substitute, as hydroxyapatite is one of the major constituents of hard tissue.

Results

Porous polymer matrices: Porous polyglycolide can be prepared by solid-state reaction from halogenoacetates, followed by extraction of the salt thus formed with water. The principal reaction scheme is given in Equation (1) for the case of sodium chloroacetate. This reaction is possible with



many halogenoacetates of the general formula $\text{X}-\text{CH}_2-\text{COOM}$. The extracted salt leaves behind a highly porous matrix of pure polyglycolide. By choice of the appropriate precursor and reaction conditions it is possible to adjust the average pore size to 0.3–1.5 μm and the porosity to 42–62 vol%. The pores are all interconnected.^[11, 12]

It is possible to prepare larger objects of this highly porous material.^[11] Pellets of 13 mm diameter and approximately 1 mm thickness were prepared with a standard IR press and

[*] Priv.-Doz. Dr. M. Epple, Dipl.-Chem. K. Schwarz
Institute of Inorganic and Applied Chemistry, University of Hamburg
Martin-Luther-King-Platz 6
D-20146 Hamburg (Germany)
Fax: (+49) 40-4123-6348
E-mail: epple@xray.chemie.uni-hamburg.de

brought into a U-tube between two aqueous solutions (see Figure 1). Each side contained an aqueous solution with one or more components of the desired precipitate. As diffusion from both sides into the pellet occurred, the components met in the pellet and formed a precipitate. Note that polyglycolide

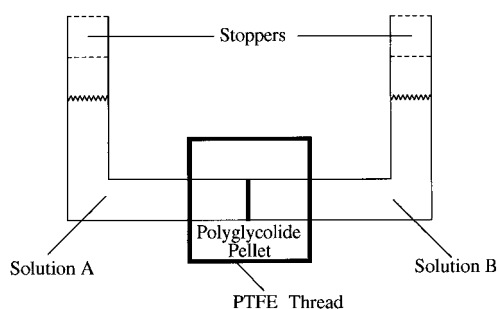


Figure 1. Schematic diagram of the experimental apparatus. A porous polymer pellet is fixed between two solutions containing the components of the precipitate. Precipitation occurs in the pellet.

is hydrophilic (contact angle with pure water $26(7)^{\circ}$ ^[19]), and that the sample is completely wet. The solubility of polyglycolide in almost all solvents is negligible, therefore the pellet is stable even after weeks in the apparatus. However, under strongly acidic or particularly alkaline conditions, hydrolysis of the ester bond occurs. This process was slow in our experiments (see Table 1).

Crystallization of fluoroapatite: In each pellet, we observed different precipitation regions. Figure 2 shows the inside of a polyglycolide pellet that was kept for 14 days at RT between two solutions (case A, see Experimental Section). No buffer was employed. Both solutions were slightly acidic (pH 5–6) throughout the experiment. The pellet was fractured after the crystallization experiment for morphological examination. Only minor amounts of fluoroapatite were deposited, as the mass of the pellet did not noticeably change. Figure 2a shows an area where small fluoroapatite crystals precipitated, widely

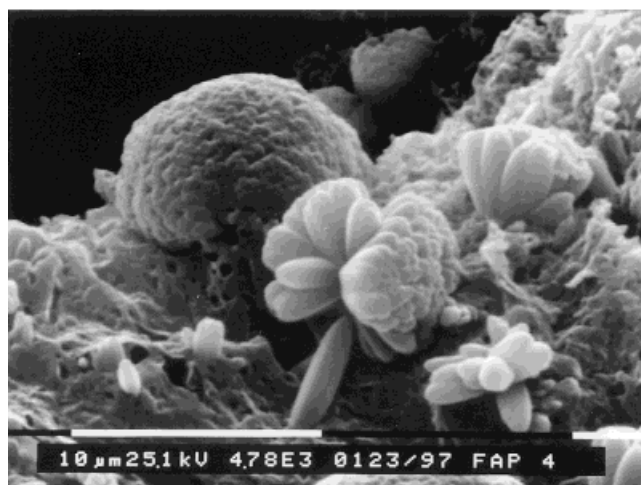
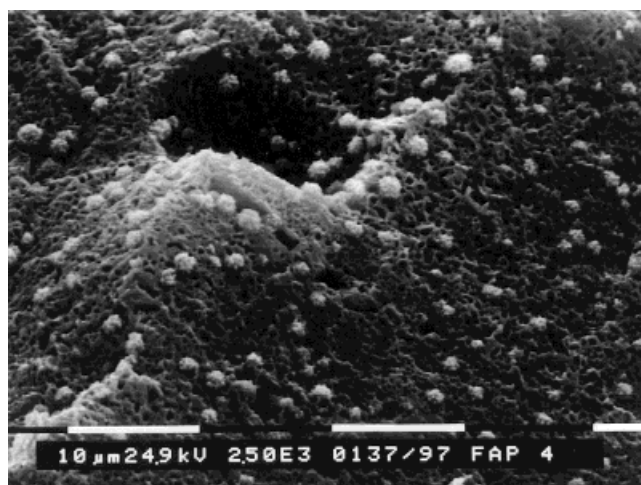


Figure 2. Fluoroapatite aggregates crystallized in a porous polyglycolide matrix over 14 days in an unbuffered environment (RT, pH about 7). The polyglycolide matrix was not removed. a) It is clearly visible that crystallization does not occur in all pores but that the aggregates are distributed over the whole surface at considerable distance from each other (magnification: $\times 2500$); b) another region of the same sample: needles of fluoroapatite start to crystallize in the pores (lower left region). From each nucleus, a bundle of needles grows to form dumbbell-shaped aggregates (right region). In later stages, the dumbbells assume a closed surface on which the original needles are still visible (upper left region) (magnification: $\times 4780$).

Abstract in German: *Hydroxylapatit und Fluorapatit wurden jeweils mit einer Doppeldiffusionstechnik aus zwei wässrigen Lösungen kristallisiert. Als Matrix diente eine Tablette aus poröser Polyhydroxyessigsäure (Polyglycolid). Die abgeschiedenen Calciumphosphat-Phasen weisen eine besondere Morphologie auf, die spezifische Wechselwirkungen zwischen den wachsenden Kristallen und der polymeren Matrix nahelegt (Keimbildungs- und Kristallwachstumsprozesse). Fluorapatit kristallisierte in verlängerten hexagonalen Prismen, deren Enden mit zunehmendem Alter des Kristalls ausfächerten, bis schliesslich geschlossene Kugeln entstanden. Hydroxylapatit wurde aus simulated body fluid (SBF) abgeschieden, einer künstlichen Lösung, deren Ionenkonzentration der des menschlichen Blutplasmas entspricht. Dabei bildeten sich hexagonale Terrassen und kompakte verlängerte hexagonale Prismen. Solche Verbundwerkstoffe aus einem bioresorbierbaren Polymer und einer Apatit-Phase sind als potentielle Biomaterialien von Interesse, beispielsweise als Knochenersatz.*

scattered over the surface (note the porous structure of polyglycolide with pore sizes of approximately $0.5\text{--}1\ \mu\text{m}$). Nucleation apparently occurred only in some regions, a fact that led to considerable distances between the particles (approximately $3\text{--}8\ \mu\text{m}$). We assume that this was a result of a decrease of the local supersaturation that was itself caused by the precipitation, so that no other nuclei can form in the close vicinity of an aggregate. Figure 2b shows another region of the same sample where the aggregates apparently had more time to mature. The crystallization began in polyglycolide pores, as indicated by needles that stick out of these voids (see lower left region). The nuclei formed bundles of needles that all started from one point (right region). Finally, dumbbell shapes developed that still show the original needles on the surface. It appears as if these dumbbells were

not closed to spheres but lay on the polyglycolide matrix. This observation points to a delicate interplay between nucleation and growth phenomena.

If concentration (case B, see Experimental Section), temperature and crystallization time were increased, fluoroapatite crystallized in larger aggregates. Figure 3 shows the inside of a polyglycolide pellet that was kept for 26 days at 37 °C in an acetate-buffered environment (pH 4.8). The polyglycolide matrix was not removed; however, it is no longer visible in Figure 3. It is possible that the polyglycolide was incorporated into the fluoroapatite matrix (like the collagen matrix in the experiments of Kniep and Busch^[1]). When the pellet was removed from the U-tube, it had softened somewhat.

Figure 3a shows elongated hexagonal prisms that formed out of one point and grew together to some extent. In other regions (Figure 3b), the prisms branched into dumbbell-shaped aggregates that closely resembled those found by Kniep and Busch.^[1] Finally, the dumbbells closed into spheres of about 60 μm diameter that completely cover the surface of the fracture (Figure 3c). The whole sample, including the

closed spheres and the dumbbells, is covered by small needles (see Figure 3d) that have diameters in the sub- μm range. This growth morphology was also observed by Kniep and Busch after the spheres had closed and underwent radial growth. This second growth stage consists of almost parallel radial growth of fluoroapatite that grow radially into the solution. Apparently, the sample was completely covered by this lawn. In some regions, this coverage was broken (e.g., Figure 3c, lower right corner), probably due to mechanical disruption as the pellet was handled.

Crystallization of hydroxyapatite from simulated body fluid:

Simulated body fluid (SBF) is a metastable aqueous solution consisting of inorganic ions in the same concentrations as in human blood plasma (see Experimental Section).^[20] The extent of deposition of calcium phosphate phases from this solution is generally considered as an indication of the biocompatibility or bioactivity of potential biomaterials, for example, ceramics, bioglasses, or polymers.^[20–28] The appropriate salts of SBF were filled into the two sides of the U-tube,

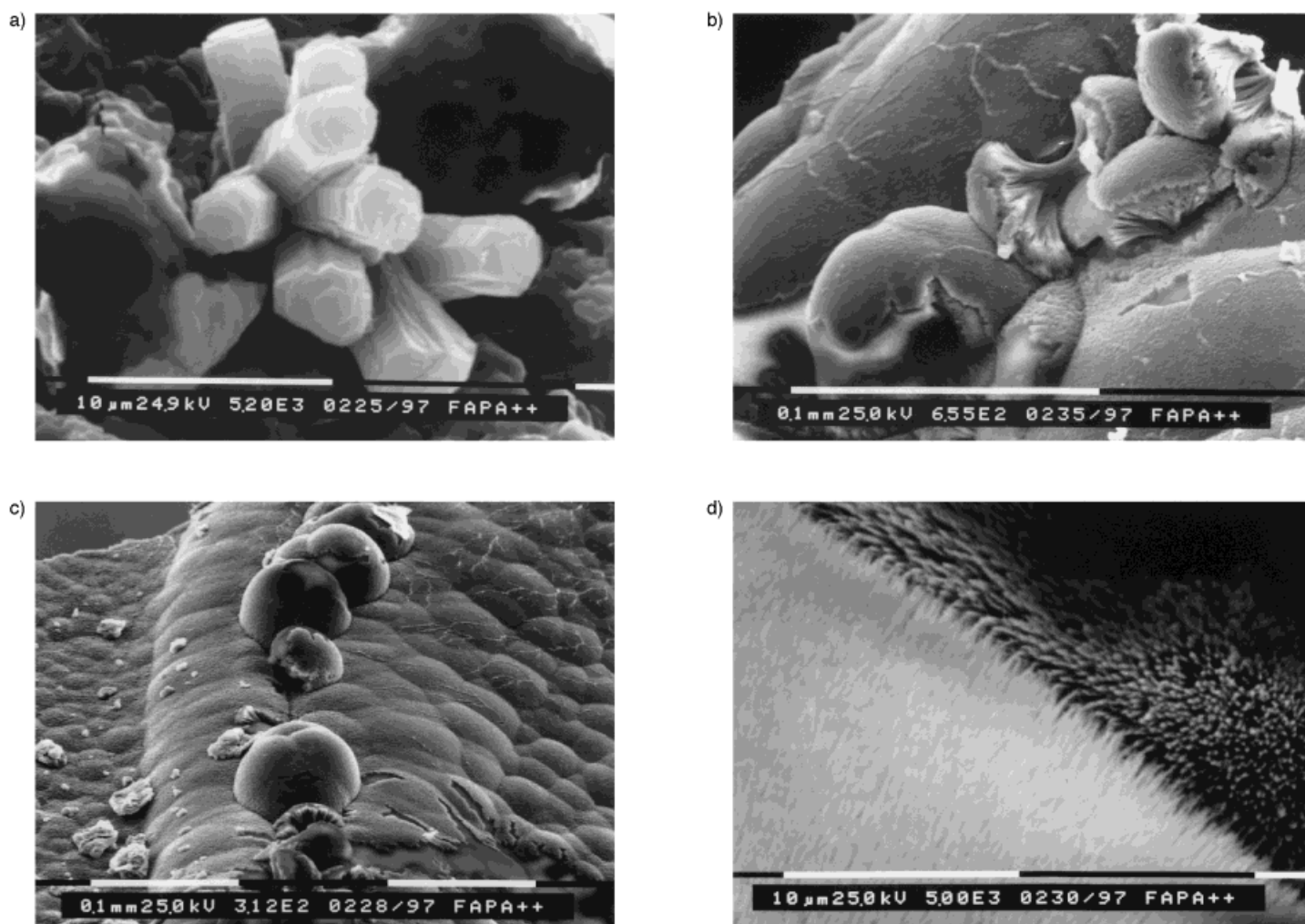


Figure 3. Fluoroapatite crystallized in a porous polyglycolide matrix over 26 days in a buffered environment (37 °C, acetate buffer, pH 4.8). Note that all pictures were taken from the same sample, but in different regions. The polyglycolide matrix was not removed. a) Elongated hexagonal prisms appear to grow out of a single nucleation site (magnification: $\times 5200$); b) in other regions, the prisms assume a branched fractal growth, very similar to that reported by Kniep and Busch^[1] (magnification: $\times 655$); c) at later growth stages, the branched prisms have closed into spheres that pack densely in the matrix (magnification: $\times 312$); d) magnification of c); on the surface of closed spheres, radial crystal growth as fine needles with sub- μm diameter occurs. The picture was taken at an edge where two spheres met (magnification: $\times 5000$).

so that the SBF ions should be present inside the pellet (where both solutions meet). No fluoride is present, therefore we expect deposition of fluoride-free hydroxyapatite instead of fluoroapatite. Note that hydroxyapatite from SBF can contain many substituting ions, as these are present in solution, and as the apatite lattice is able to accommodate many other anions and cations.^[29] Most authors have identified the precipitate from SBF as carbonated hydroxyapatite (see, e.g., refs. [22, 26]). However, its composition strongly depends on the local pH.^[28]

Figure 4 shows apatite aggregates that were found inside a pellet that was kept for 26 days at 37 °C (unbuffered environment). The polyglycolide matrix was removed by calcination at 500 °C. Again, different regions were found in the pellet. Flat hexagonal prisms grew in a regular, terrace-shaped morphology resembling human bone structures (although much larger).^[2] In other regions of the same pellet, apatite crystallized as elongated hexagonal prisms, again starting from one nucleation point (see the upper left corner of Figure 4b). The prisms close into almost spherical aggregates. On their surface they still show the tops of the elongated prisms (see right side of Figure 4b). This growth morphology is different from that found for fluoroapatite (see above), despite the fact that the elongated prisms finally close up to form spheres. Here, no fractal growth with decreasing needle diameter and increasing number of needles is observed, but simple growth of interlinked hexagonal prisms from a common nucleation site finally leads to a quasispherical surface.

Discussion

The results of the precipitation experiments are summarized in Table 1. A major deposition of apatite is observed only at 37 °C and after approximately 4 weeks. However, small spherical aggregates can be detected after one week. This points to a kinetic limitation of the crystallization that influences diffusion, nucleation, and crystal growth.

Both fluoroapatite and hydroxyapatite exhibit distinct crystal shapes upon crystallization in porous polyglycolide matrixes. The aggregates are much larger than the maximum pore diameter of the polymer, so it is obvious that apatite nuclei, once formed in a pore, grow by pushing the poly-

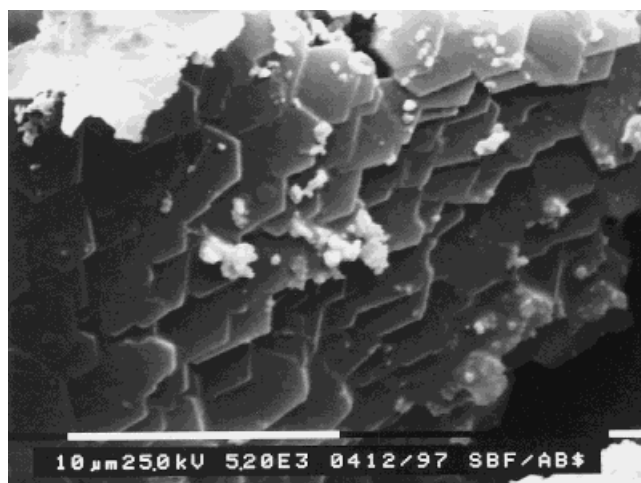


Figure 4. Hydroxyapatite crystallized from simulated body fluid over 26 days (37 °C, unbuffered environment, pH about 7). The polyglycolide matrix was removed by heating to 500 °C; a) interlinked hexagonal prisms that assume terrace-shaped morphology (magnification: $\times 5200$); b) spherical aggregates that have grown out of elongated hexagonal prisms (right); a younger aggregate is visible in the upper left part (magnification: $\times 1310$).

glycolide matrix away. The system has many potential nucleation sites, as the pores account for about 43 vol% of the pellet (however, not all sites are actually occupied by apatite, as Figure 2a shows). The formed nuclei grow to larger

Table 1. Summary of precipitation experiments of fluoroapatite and hydroxyapatite from simulated body fluid. Negative mass balances are due to partial hydrolysis of the polyglycolide matrix. Dimensions of spherical aggregates are given as average diameters.

Sample	Condi-tions	<i>T</i>	<i>t</i>	pH	Observed morphology	Mass change of pellet after ex-periment
fluoroapatite	case B	RT	7 days	ca. 5	few spheres only (ca. 3–8 μm)	no change
fluoroapatite	case A	RT	13 days	4.8 (acetate buffer)	spheres only (ca. 10 μm)	+ 6 wt %
fluoroapatite	case A	RT	13 days	ca. 5	spheres only (ca. 3–8 μm)	– 3 wt %
fluoroapatite (Figure 2)	case A	RT	14 days	ca. 6	spheres only (ca. 3–8 μm)	no change
fluoroapatite (Figure 3)	case B	37 °C	26 days	4.8 (acetate buffer)	elongated hexagonal prisms (ca. 4 × 10 μm); dumbbell-shaped aggregates; closed spheres (ca. 60 μm); radial growth	+ 50 wt %
hydroxyapatite (Figure 4)	SBF	37 °C	26 days	ca. 7	hexagonal terraces; hexagonal prisms (ca. 5 × 40 μm); spherical aggregates (ca. 50 μm)	+ 30 wt %

aggregates that are often linked together, in contrast to those in the experiments carried out by Kniep and Busch, who used a system with fewer nucleation sites.^[1]

It may be assumed that the endgroups of the polymer are preferentially found at the surface of the polymer where they would cause minimal disruption of the highly crystalline polymer structure. Consequently, the inside of the pores would be covered by carboxy and hydroxy endgroups (as identified earlier by in-situ IR spectroscopy: $\text{HOOC-CH}_2\text{-[-OOC-CH}_2\text{-]}_n\text{-OH}$ ^[30]). It makes sense to assume that such carboxy groups can induce nucleation of apatite, because it is well known that carbonate can be substituted for hydroxide or phosphate in the apatite lattice.^[29] Li et al. proposed that carboxy groups of a polyester were responsible for the nucleation of calcium phosphate from SBF.^[27] Crystallization of apatite from SBF on porous silica gels indicated that nucleation is induced by silanol (Si-OH) groups.^[22, 23] It is reasonable to assume that polyglycolide is able to induce crystallization from supersaturated calcium phosphate solutions by means of carboxy and hydroxy groups on its (internal) surface.

Deposition of hydroxyapatite from SBF was also observed on calcium phosphate ceramics that are developed as bioactive biomaterials.^[20, 21, 24, 26, 27] Frequently, spherical aggregates were found that are often interconnected and generally covered with a hairy layer of apatite. Examples of substrates are a polyethylene oxide-polybutylene terephthalate copolymer (diameter 20 μm),^[27] titania and its alloys (diameter 10 μm),^[25] porous silica (diameter 10 μm),^[23] Na-Ca-Al-phosphate glasses (diameter 3 μm),^[26] collagen fibers (diameter 5–10 μm),^[31] and Ca-Si-La/Y-O glasses (diameter 0.5–5 μm , depending on the substrate)^[24] (the typical diameter of the aggregates is given in parentheses). Interestingly, hydroxyapatite from pulsed laser deposition on titanium also gave intergrown globules of about 3 μm diameter that were themselves composed of smaller units (150–250 nm diameter).^[32] We may therefore conclude that an arrangement of spherical, hairy crystals is to some extent typical for the crystallization of hydroxyapatite on surfaces. This stands in contrast to the solid, compact aggregates that we have found for hydroxyapatite.

It is very difficult to quantitatively interpret the results that were obtained by the diffusion experiments. Firstly, it is clear that different regions exist in each pellet. These regions presumably contain apatite crystals of different age. A plausible model can be formulated as follows. The very first crystals are formed in the center of the pellet where the two solutions meet at the beginning of the experiment. The precipitation is induced by surface groups of polyglycolide. In the immediate vicinity of a growing crystal, the solution is depleted of solute and further nucleation is inhibited, leading to separated nuclei (see Figure 2a). As the crystals grow, they push away the polyglycolide matrix. This creates cracks in the pellet through which further mixing of the two solutions can occur. This in turn gives a local supersaturation beyond the initial precipitation zone in the center, creating further nuclei. At this stage, the cycle starts again. The pores, although interconnected, are not directionally oriented, therefore the precipitation and cracks are expected to occur in many

directions, leading to a fuzzy interface between the two solutions. The oldest and largest aggregates are expected in the initial precipitation zone (see Figures 3a–d).

It is known that the crystallization of apatites^[29] is influenced by a variety of variables: presence of ions^[33] such as fluoride,^[34] pore size (nm range) of substrates,^[22] and pH.^[28] Of course, the local supersaturation plays a major role as well. In our system, we are able to control some external parameters (temperature, pH outside the pellet, concentrations outside the pellet). In contrast, it is not possible to control the local conditions inside the pellet where precipitation must lead to local concentration changes and apatite crystallization leads to a decrease in local pH. This must cause locally and temporarily different rates of nucleation and crystal growth that are very difficult to estimate.

Conclusions

The results shown above demonstrate that calcium phosphate phases are formed in specific biomimetic morphology by diffusion of two solutions into a porous polyglycolide matrix. The situation is complex, but it appears clear that polyglycolide acts as specific environment that directs nucleation and growth of both hydroxyapatite and fluoroapatite to give such a special morphology. In contrast to collagen, polyglycolide does not have a polar structure (see ref. [35] for its crystal structure); therefore we rule out a dipolar electrostatic interaction^[1] between fluoroapatite and the matrix as the reason for the special growth morphology. Further experiments with variation of external (temperature, time, pH, concentration, additives, surfactants) and internal (pore size, thickness of pellet) parameters are necessary to understand these processes. If we knew how to control the crystallization, we would be able to prepare a polyglycolide pellet completely filled with micrometer-sized apatite crystals, a promising composite as bone replacement material.^[16]

Experimental Section

Polyglycolide was prepared from previously ground sodium chloroacetate as described in ref. [10]. Briefly, sodium chloroacetate was thermally converted to polyglycolide and NaCl and compacted to a pellet, and the sodium chloride was extracted with cold water. Inorganic salts were used in pro analysi quality. Fluoroapatite was precipitated from two solutions that were used to fill the two compartments of a U-tube. Two sets of concentrations were employed; the first one corresponded to the conditions used by Kniep and Busch:^[1] 133 mM CaCl_2 with 80 mM Na_2HPO_4 and 27 mM KF (case A). In the second case, we used higher concentrations: 186 mM CaCl_2 with 110 mM Na_2HPO_4 and 38 mM KF (case B).

Simulated body fluid (SBF) with an ion concentration close to human blood plasma was prepared according to ref. [20] (slightly improved concentrations). One side of the U-tube contained the following components: Na_2HPO_4 2 mM, KHCO_3 5 mM, KCl 2 mM, MgSO_4 1 mM, MgCl_2 1 mM, NaHCO_3 49 mM, NaCl 89.5 mM; the other KCl 3 mM, MgCl_2 1 mM, CaCl_2 5 mM, NaCl 140.5 mM. Thus, SBF would be formed if both compartments were completely mixed. After such (hypothetical) mixing, one would obtain the following SBF concentration (values for human blood plasma in parentheses): Na^+ 141.5 mM (142 mM), K^+ 5 mM (5 mM), Mg^{2+} 1.5 mM (1.5 mM), Ca^{2+} 2.5 mM (2.5 mM), Cl⁻ 124.5 mM (103 mM), HCO_3^- 27 mM (27 mM), HPO_4^{2-} 1 mM (1 mM), and SO_4^{2-} 0.5 mM (0.5 mM). Complete

mixing does not occur, but it is reasonable to assume the final concentrations at the precipitation zone within the pellet.

After the experiment, the pellets were carefully removed from the U-tube, rinsed with deionized water and dried at 50 °C. Examinations were made at fracture planes inside each pellet. A representative section of each pellet was calcined at 500 °C and the remaining inorganic precipitate was analyzed by X-ray powder diffraction. In cases where a sufficient amount of precipitate had been deposited, we also took a powder diffractogram of the ground apatite together with its polymeric matrix. In the case of the fluoroapatite deposition, differentiation between hydroxyapatite and fluoroapatite is almost impossible by conventional XRD, as the cell dimensions and the scattering power are practically identical. In addition, partial substitution of hydroxide by fluoride is possible to any extent. As a consequence, it is not known how much hydroxide is contained in the precipitated fluoroapatite.

All pellets were weighed before and after the experiment. In most cases, except for the experiments at 37 °C, the mass difference was small. Note that the deposition of apatite was partially compensated by slow hydrolysis of polyglycolide, which in some cases even led to a mass loss.

For X-ray powder diffraction we used a Philips PW1050/25 diffractometer with nickel-filtered $\text{Cu}_{K\alpha}$ radiation ($\lambda = 154.178$ pm) equipped with a proportional detector. Scanning electron microscopy was performed with a Philips SEM 515 instrument operating at 25 kV with gold-sputtered samples. Calcium phosphate phases were also identified by energy-dispersive X-ray spectroscopy (EDX).

Acknowledgments: We are grateful to Prof. A. Reller for generous support. We thank B. Hasse and M. Plughoefft for assistance with experiments and Prof. H. Lechert for permission to use the scanning electron microscope. This work was supported by the Fonds der Chemischen Industrie and the Deutsche Forschungsgemeinschaft (Heisenberg grant for M.E.).

Received: February 17, 1998 [F 1010]

- [1] R. Kniep, S. Busch, *Angew. Chem.* **1996**, *108*, 2788–2791; *Angew. Chem. Int. Ed. Engl.* **1996**, *35*, 2624–2626.
- [2] S. Mann, *Biomimetic Materials Chemistry*, VCH, Weinheim, **1996**.
- [3] P. Calvert, P. Rieke, *Chem. Mater.* **1996**, *8*, 1715–1727.
- [4] G. A. Ozin, H. Yang, I. Sokolov, N. Coombs, *Adv. Mater.* **1997**, *9*, 662–667.
- [5] S. Weiner, L. Addadi, *J. Mater. Chem.* **1997**, *7*, 689–702.
- [6] S. I. Stupp, P. V. Braun, *Science* **1997**, *277*, 1242–1248.
- [7] J. Aizenberg, J. Hanson, T. F. Koetzle, S. Weiner, L. Addadi, *J. Am. Chem. Soc.* **1997**, *119*, 881–886.
- [8] G. Falini, S. Fermani, M. Gazzano, A. Ripamonti, *Chem. Eur. J.* **1997**, *3*, 1807–1814.
- [9] J. M. Marentette, J. Norwig, E. Stöckelmann, W. H. Meyer, G. Wegner, *Adv. Mater.* **1997**, *9*, 647–651.
- [10] M. Epple, H. Kirschnick, *Chem. Ber.* **1996**, *129*, 1123–1129.
- [11] M. Epple, O. Herzberg, *J. Mater. Chem.* **1997**, *7*, 1037–1042.
- [12] M. Epple, O. Herzberg, *J. Biomed. Mater. Res.* **1998**, *43*, 83–88.
- [13] G. O. Hofmann, *Arch. Orthopaed. Trauma Surg.* **1995**, *114*, 123–132.
- [14] E. Chiellini, R. Solaro, *Adv. Mater.* **1996**, *8*, 305–313.
- [15] C. K. Breuer, T. Shin'oka, R. E. Tanel, G. Zund, D. J. Mooney, P. X. Ma, T. Miura, S. Colan, R. Langer, J. E. Mayer, J. P. Vacanti, *Biotechnol. Bioeng.* **1996**, *50*, 562–567.
- [16] K. C. Dee, R. Bizios, *Biotechnol. Bioeng.* **1996**, *50*, 438–442.
- [17] H. Winet, J. Y. Bao, *J. Biomater. Sci. Polymer Ed.* **1997**, *8*, 517–532.
- [18] N. Ashammakhi, P. Rokkanen, *Biomaterials* **1997**, *18*, 3–9.
- [19] R. Kapur, B. J. Spargo, M. S. Chen, J. M. Calvert, A. S. Rudolph, *J. Biomed. Mater. Res.* **1996**, *33*, 205–216.
- [20] O. P. Filho, G. P. LaTorre, L. L. Hench, *J. Biomed. Mater. Res.* **1996**, *30*, 509–514.
- [21] P. Li, C. Ohtsuki, T. Kokubo, K. Nakanishi, N. Soga, K. de Groot, *J. Biomed. Mater. Res.* **1994**, *28*, 7–15.
- [22] M. M. Pereira, A. E. Clark, L. L. Hench, *J. Am. Ceram. Soc.* **1995**, *78*, 2463–2468.
- [23] S. B. Cho, K. Nakanishi, T. Kokubo, N. Soga, C. Ohtsuki, T. Nakamura, T. Kitsugi, T. Yamamuro, *J. Am. Ceram. Soc.* **1995**, *78*, 1769–1774.
- [24] R. Fresa, A. Costantini, A. Buri, F. Branda, *Biomaterials* **1995**, *16*, 1249–1253.
- [25] T. Kokubo, F. Miyaji, H. M. Kim, *J. Am. Ceram. Soc.* **1996**, *79*, 1127–1129.
- [26] L. J. Jha, J. D. Santos, J. C. Knowles, *J. Biomed. Mater. Res.* **1996**, *31*, 481–486.
- [27] P. Li, D. Bakker, C. A. van Blitterswijk, *J. Biomed. Mater. Res.* **1997**, *34*, 79–86.
- [28] J. Li, H. Liao, M. Sjöström, *Biomaterials* **1997**, *18*, 743–747.
- [29] J. C. Elliot, *Structure and Chemistry of the Apatites and Other Calcium Orthophosphates*, Elsevier, Amsterdam, **1994**.
- [30] M. Epple, H. Kirschnick, J. M. Thomas, *J. Therm. Anal.* **1996**, *47*, 331–338.
- [31] Y. Doi, T. Horiguchi, Y. Moriwaki, H. Kitago, T. Kajimoto, Y. Iwayama, *J. Biomed. Mater. Res.* **1996**, *31*, 43–49.
- [32] C. K. Wang, J. H. Chern Lin, C. P. Ju, H. C. Ong, R. P. H. Chang, *Biomaterials* **1997**, *18*, 1331–1338.
- [33] P. W. Brown, M. Fulmer, *J. Biomed. Mater. Res.* **1996**, *31*, 395–400.
- [34] M. Iijima, D. G. A. Nelson, Y. Pan, A. T. Kreinbrink, M. Adachi, T. Goto, Y. Moriwaki, *Calcif. Tissue Int.* **1996**, *59*, 377–384.
- [35] Y. Chatani, K. Suehiro, Y. Okita, H. Tadokoro, K. Chujo, *Makromol. Chem.* **1968**, *113*, 215–229.